Supplementary Information

A Flexible Pyro-phototronic Nanogenerator based on Surface-Polarization Effect

Shakyadeep Bora,[a,b] Jyotisman Bora,[a] Khomdram Bijoykumar Singh,[a,b] Bablu Basumatary,[a,c] Deepshikha Gogoi,[a,d] and Arup Ratan Pal*, [a,b]

[a]Plasma Nanotechnology Laboratory, Physical Sciences Division, Institute of Advanced Study in Science and Technology, Paschim Boragaon, Garchuk, Guwahati – 781035

[b]Academy of Scientific and Innovative Research (AcSIR), Ghaziabad- 201002, India

[c] Department of Physics, Dimoria College, Khetri, Kamrup, Assam 782403, India

[d]Department of Physics, Abhayapuri College, Bongaigaon 783384, India

E-mail: arpal@iasst.gov.in

Contents

Figure S1: Photograph of the flexible nanogenerator device

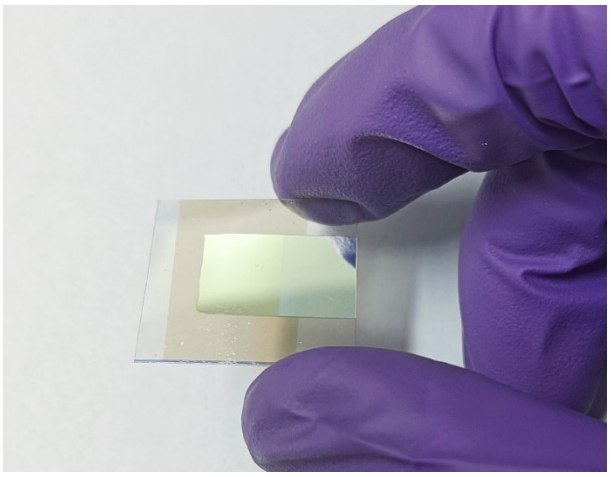

Figure S2: UPS and VBS spectra of the PPA-CRB device showing SECO (Secondary electron Cut-off), Fermi energy edge (E_F), edges of HOMO (VB) and LUMO (CB) levels.

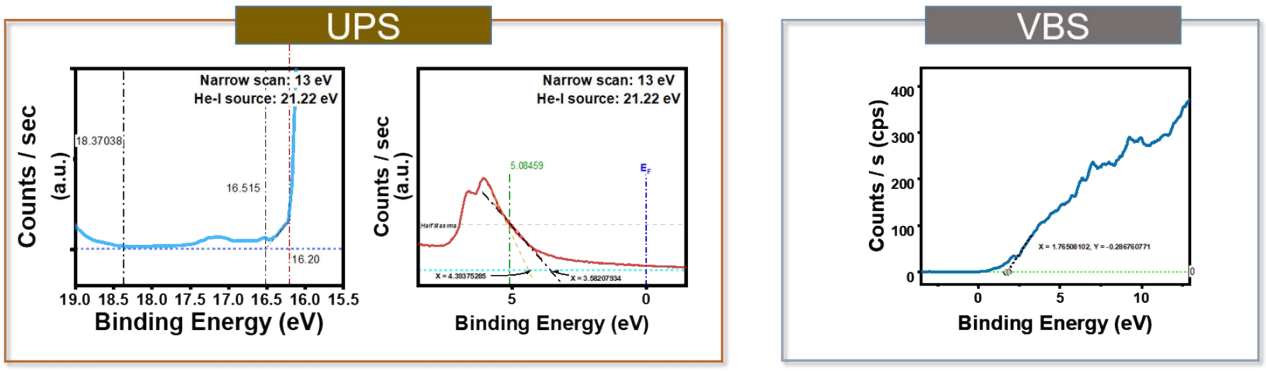

Figure S3: UV- Visible spectrum of as-synthesised PPA-CRB (plasma-polymerised aniline – crystalline rubrene) thin film.

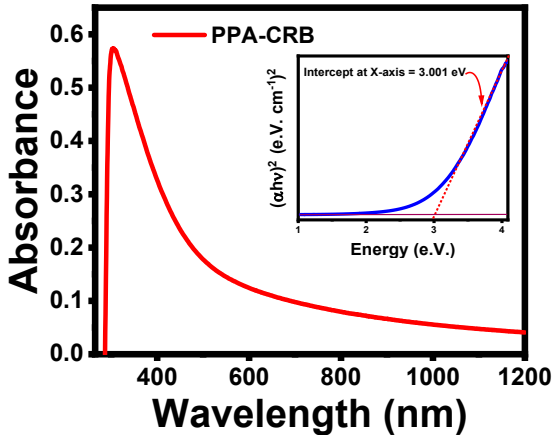

--

Table T1: Raman spectrum peak positions of PPA-CRB with band assignment values.

Material	Raman Shift (cm^{-1})	Assignments
PPA-CRB	1034	Amine deformation (C-N-C) bending
	1162	C-H bending deformation of Quinoid ring
	1190	Rubrene film
	1218	Rubrene crystal
	1302	Rubrene crystal
	1315	Rubrene crystal
	1355	Rubrene film
	1430	C-C str quinoid vibrations

	1480	C-N str benzenoid vibration
	1500	C=C str benzenoid vibrations
	1539	C=N str quinoid vibrations
	1614	Rubrene crystal

Figure S4: I-V (current voltage) characteristics of the device under different wavelengths ranging from 365 nm to 935 nm.

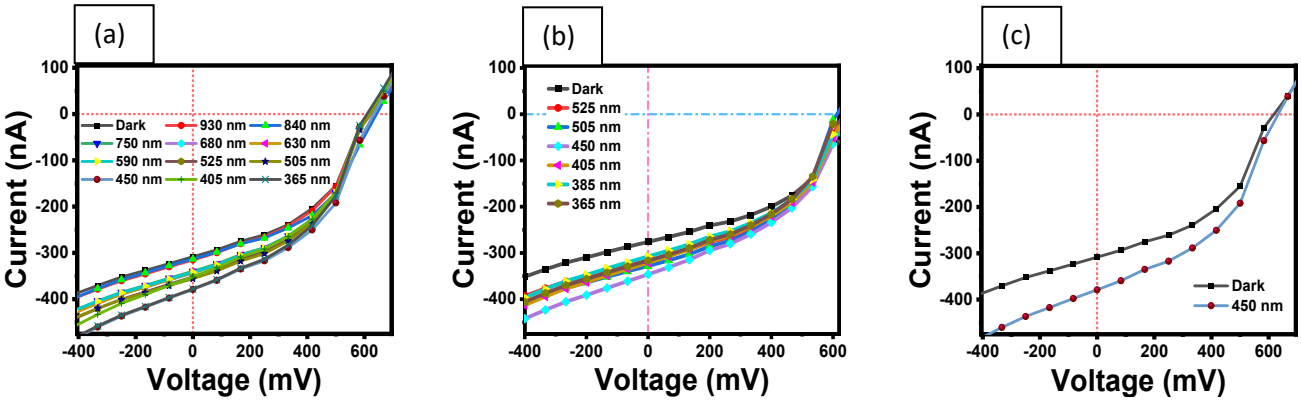

Figure S5: Responsivity of the PPA-CRB device.

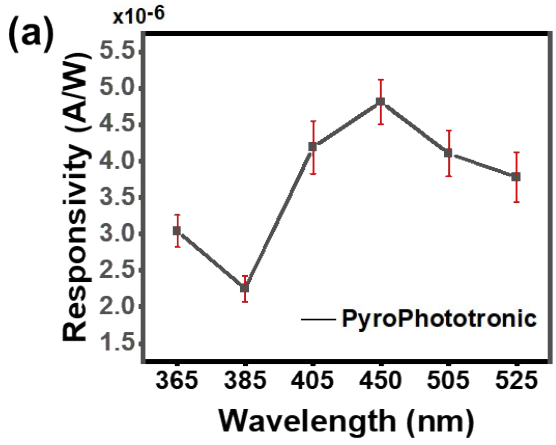

Figure S6: Open circuit temporal responses of voltage under illumination of different wavelengths at a selected range (a) 365 nm, (b) 385 nm, (c) 405 nm, (d) 450 nm, (e) 505 nm, and (f) 525 nm.

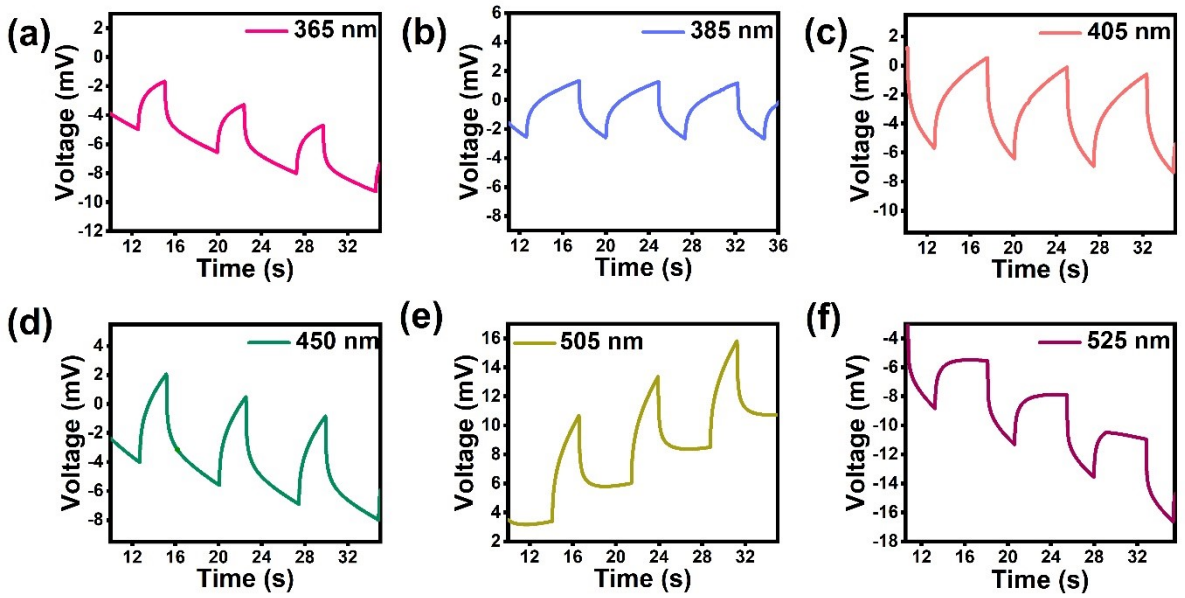

Figure S7: Thermal images of the PPA-CRB on glass under different light intensities of (a) 0.5 mWcm^{-2} and (b) 1.0 mWcm^{-2}

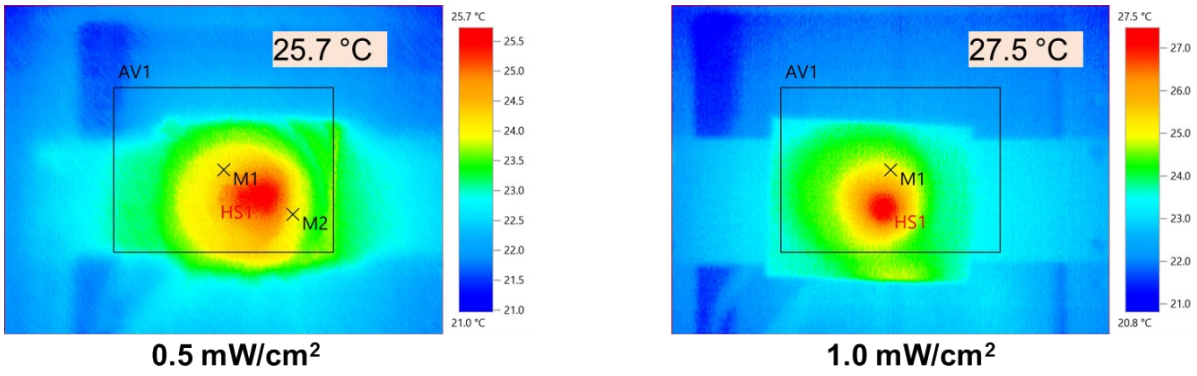

Figure S8: Schematic shows normal pyro-phototronic charge dynamic mechanism in terms of energy level diagram without any bending condition.

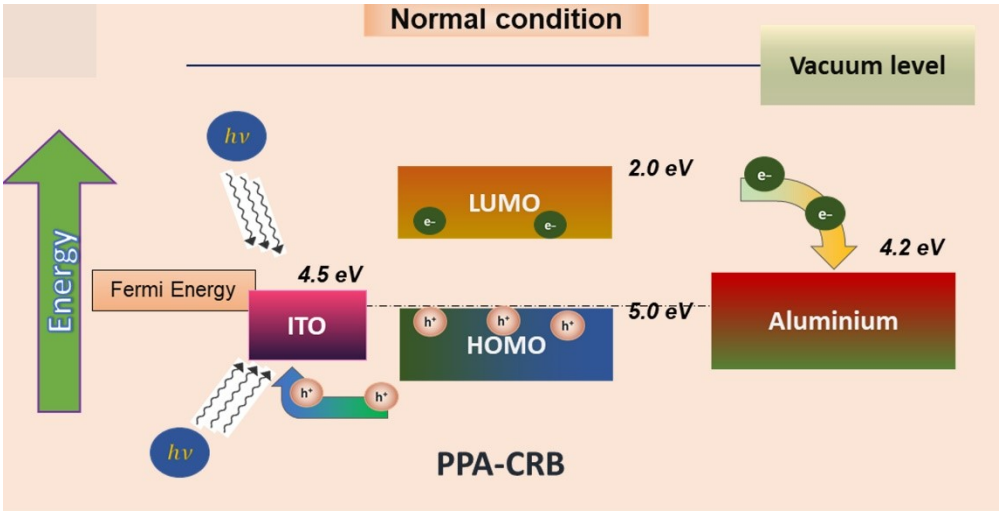

Table T2: All the formulae used in the main text / manuscript for calculating various parameters.

Sl No.	Parameter	Formulae Used	Description
(i)	Spectral Responsivity	$R_\lambda = \frac{I_\lambda}{P_\lambda \times A}$	Ratio of photocurrent to product of incident power & surface area
(ii)	Pyroelectric coefficient	$p = \frac{I_p}{A} \times \frac{dt}{dT}$	Ratio of pyroelectric current to pyroelectric active area divided by temperature difference w.r.t. time
(iii)	Curvature of a surface	$K = \frac{1}{R}$	Reciprocal of radius of the surface
(iv)	Surface Power Density	$\frac{P}{A} = \frac{(I_{pyro+photo} \times V_{pyro+photo})}{Area}$	Product of peak to peak pyrophototronic current and voltage (self-powered mode) per unit area
(v)			

References

(1) D. Gogoi, S. Podder, J. Bora, S. Biswasi and A. R. Pal, *Opt. Mater.*, 2021, **122**, 111733.

(2) K. P. Dhakal, J. Joo and J. Kim, *Curr. Appl. Phys.*, 2022, **39**, 304.

(3) S. W. Park, J. M. Choi, K. H. Lee, H. W. Yeom, S. Im and Y. K. Lee, *J. Phys. Chem. B*, 2010, **114**, 5661.

(4) B. Basumatary, D. Gogoi, S. Podder, J. Bora, K. B. Singh, S. D. Bora, A. R. Pal and D. S. Patil, *Nano Energy*, 2023, **114**, 108655.

(5) S. Biswasi, D. Gogoi and A. R. Pal, *Appl. Surf. Sci.*, 2022, **599**, 153883.

(6) J. Bora, S. Podder, D. Gogoi, B. Basumatary and A. R. Pal, *J. Alloys Compd.*, 2021, **879**, 160460.